

# Rayleigh Fading with Modified Poisson Time Arrival Path in OFDM Smart Antennas for WLAN Underground Communications

Salma AIT FARES<sup>(1,2)</sup>, Tayeb A. DENIDNI<sup>(1,2)</sup>, Sofiène AFFES<sup>(1,2)</sup>, and Charles DESPINS<sup>(1,2,3)</sup>

1: INRS- EMT, Place Bonaventure, 800 de la Gauchetiere Ouest, suite 6900  
Montreal, Qc, Canada, H5A1K6

Tél: (514) 875-1266 ext 2017. Fax: (514) 875-0344.

2: UNDERGROUND Communications Research Laboratory (LRCS), Val d'or, Qc, Canada

3: Prompt-Québec, Montreal, Canada

Email :{ aitfares, denidni, affes } @ inrs-emt.quebec.ca, cdespins@promptquebec.com

## ABSTRACT

Most analytical studies of orthogonal frequency division multiplexing (OFDM) smart antennas with channel fading assume a constant number of multiple paths. In certain wireless applications, such as indoor and underground environments, the number of the significant multipath components can be variable and follows a specific distribution. Based on statistical modeling of a wideband radio propagation channel in our mining environment, it turned out that the number of arrival paths and their amplitudes follow a modified Poisson distribution and undergo Rayleigh fading. In this paper, the impact of Rayleigh fading and modified Poisson distribution for the path arrival on antenna-array systems with OFDM modulation is investigated. A comparative study of antenna array architectures using pre-FFT and post-FFT processing and the dependency of the channel characteristics for each array processing are presented. The bit-error rate for different conditions is evaluated for comparison purposes.

## 1. INTRODUCTION

Orthogonal Frequency Division Multiplexing (OFDM), which is a modulation technique for multi-carrier communication systems, has many advantages over a single carrier for high data rate transmission in multipath fading channels. One of the main reasons for the use of OFDM is to increase system robustness against frequency selective fading or narrowband interferences. Recently, adaptive antenna arrays (AAA) have been used in OFDM systems. These techniques have been of interest because of OFDM's ability to combine multipath signals and suppress interference [1-3]. Spatial signal processing can be applied either in the *time domain* (*pre-FFT*) or in the *frequency domain* (*post-FFT*) at the receiver. Compared with post-FFT [9,1] antenna arrays, much lower computation complexity and much shorter training sequences are required in the pre-FFT [8] antenna array schemes [2,3], at a cost of slight performance degradation.

The design of appropriate combining schemes as well as the system performance crucially depend on the channel fading characteristics. However, there are relatively few technical papers on applying antenna arrays (AA) to OFDM systems while investigating the effect of channel fading characteristics on wireless communication system performance [7], and particularly on wireless underground communication environments. One major effect that deteriorates the system performance in such environments is the number of multiple

paths and the fading distribution. Multipath propagation causes delay dispersion and frequency selective fading in the time and frequency domains, respectively. In addition, most analytical studies of the performance of OFDM-AAA on fading channels assume constant number and time arrival multipath environments [7]. Based on statistical modeling of a wideband radio propagation channel in our mining environment, the number of significant multipath components is variable and follows an identifiable distribution. It has been revealed that it follows a modified Poisson distribution [4]. However, OFDM allows good robustness against frequency-selective fading due to the exploitation of a guard interval that is inserted at the beginning of each OFDM symbol. However, if delayed signals beyond the guard interval are introduced in a channel with a large delay spread, intersymbol interference (ISI) arises and causes severe performance degradation.

In this paper, the impact of Rayleigh fading and modified Poisson distribution for the path arrival in AAA WLAN OFDM systems performance is investigated. Furthermore, a comprehensive comparative study of AAA architectures using pre-FFT and post-FFT is presented, and the dependency of the channel property for each array processing is clarified. This type of study is crucial and essentially important to be carried out for the proposed OFDM –AAA system performance. The bit-error-rate (BER) performance of the OFDM system with space diversity is evaluated and the trade-off between complexity, accuracy and system capacity in this environment is also studied. Section 2 describes the OFDM channel model. Then, the concept of adaptive antenna arrays using OFDM based on pre-FFT and post-FFT is described in Section 3. In Section 4, the performance of pre-FFT array processing and post-FFT array processing are presented. Finally, Section 5 concludes this paper.

## 2. OFDM CHANNEL MODEL

### 2.1. OFDM principle

The structure of a basic OFDM communication system with  $N$  sub-carriers signalling is illustrated in Fig. 1. As shown in the block diagram, data and pilot symbols are modulated on a set of  $N$  subcarriers by combining them using Inverse Fast Fourier Transformation (IFFT). The last  $N_g$  samples of the IFFT outputs are then copied and added to form the guard interval at the beginning of each OFDM symbols. The transmitted OFDM signal in its sampled equivalent low-pass representation is given by:

$$s_l = \sum_{k=0}^{N-1} c_k \cdot e^{j2\pi k l / N}, \quad (-N_g \leq l \leq N) \quad (1)$$

where  $N_g$  is the number of symbols in the guard interval and  $c_k(k=0, \dots, N-1)$  is the associated modulated symbol of the  $k$ th subcarrier.

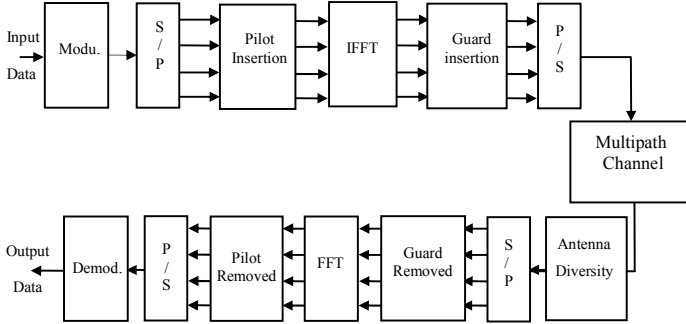


Fig.1 Block diagram of a basic OFDM communication system.

At the receiver, the reverse process takes place: The cyclic prefix is removed, the signal is converted from serial to parallel and is passed through an  $N$ -point FFT. The transmitted signal propagates through the multipath fading channels with additive noise and it is received by the diversity antennas. The received signal is then given by:

$$r_l^{(m)} = h_l^{(m)} \otimes s_l + \eta_l^{(m)} \quad (2)$$

where  $\otimes$  is the convolution operation;  $h_l^{(m)}$  is the channel impulse response (CIR) at the  $m$ -th diversity branch in its sampled equivalent low-pass form; and  $\eta_l^{(m)}$  is the additive white Gaussian noise (AWGN) component at the  $m$ th-diversity branch. We assume that  $h_i$  has a nonzero value only for the duration  $0 \leq i \leq K$  where  $K$  is the CIR length.

▪ **Pilot Arrangement**

OFDM-AAA is usually performed using pilot symbols inserted at known subcarriers in the time-frequency domain. Several kinds of pilot arrangements have been studied [10]. We consider two main pilot arrangements. The first kind shown in Fig. 2(a) is denoted as *block-type* pilot arrangement. The pilot signal is assigned to a particular OFDM block, which is sent periodically. This pilot arrangement is especially suitable for slow fading radio channels. The second kind shown in Fig. 2(b) is denoted as *comb-type* pilot. The  $N_p$  pilots are uniformly distributed within an OFDM symbol and data is assigned to other subcarriers according to the following equation:

$$X(k) = \begin{cases} x_p(m) & l = 0 \\ \text{Information data} & l = 1, \dots, L-1 \end{cases} \quad (3)$$

where  $L=N/N_p$ , and  $x_p(m)$  is the  $m$ th pilot carrier value. Since only some subcarriers contain the pilot signal, the comb-type pilot arrangement is sensitive to frequency selectivity when compared to the block-type pilot arrangement system.

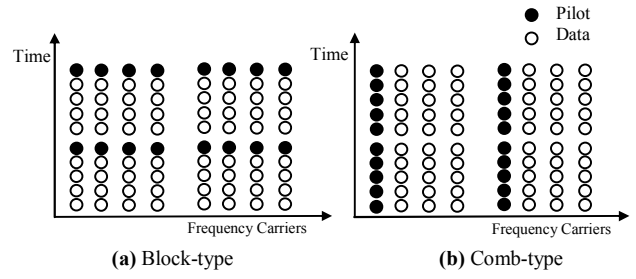


Fig.2: Two different types of pilot subcarriers arrangement.

2.2. Channel Model

The vector CIR can be represented as follows:

$$\mathbf{h}(t) = \sum_{i=1}^K A_i(t) \cdot e^{j\phi_i(t)} \cdot \mathbf{a}(\theta_i(t)) \cdot \delta(t - \tau_i(t)) \quad (4)$$

where  $A_i$ ,  $\phi_i$  and  $\tau_i$  determine the amplitude, carrier phase shift and time delay of the  $i$ th multipath.  $\mathbf{a}(\theta_i)$  is the array response vector. The amplitude  $A_i$  of the multipath component is usually modeled as a Rayleigh distributed random variable, while the phase shift  $\phi_i$  is uniformly distributed.

▪ **Path arrival model**

In indoor environments, especially underground mines, where the obstacles are completely randomly positioned, the assumption of the Poisson distribution should be adequate to model the time arrival of paths. However, the modified Poisson distribution has been conceived with an aim of filling the insufficiency of the Poisson distribution model by taking into account the path-arrival-rate of the impulses to each delay index [4].

The statistical characterization of the channel propagation in our mining environment [4-5] revealed that the path arrival times follow a modified Poisson distribution and the multipath number of the significant paths can reach fifteen with eight *nsec* resolution as shown in Fig.3.



Fig.3 Time Delay.

3. OFDM ADAPTIVE ANTENNA ARRAY

The structure of OFDM-AAA can be applied either in the *time domain* or in the *frequency domain*, namely, *pre-FFT* and *post-FFT*, respectively.

3.1. LMS Beamforming based on Pre-FFT array processing

In the pre-FFT adaptive array (AA), the received signal is multiplied by the weight of the adaptive beamformer, and then transformed back into the frequency domain by using FFT

processing. The error signal, between the pilot symbols and the corresponding received signals in the frequency domain, is transformed into the time domain by using IFFT processing, and used to update the weights of the adaptive beamformer. The weight vector  $w$  is updated by minimizing MSE criteria using the LMS algorithm. Fig.4 shows a typical architecture of pre-FFT adaptive array processing [11].

The output of the beamformer for the  $k$ th subcarrier symbol is:

$$y_k = \sum_{m=1}^M w_m^* \cdot r_k^{(m)} \quad (5)$$

where  $w_m$  is the weight of the  $m$ th branch,  $r_k^{(m)}$  is the signal of the  $k$ th subcarrier symbol received by the  $m$ th antenna, and  $M$  is the number of antenna elements.

Then the adaptation method in the following simulations uses the LMS algorithm where the reference signal is generated with a more general form than the one used in [11] in order to protect the received signal against the frequency fading. In our case, the pilots are inserted with an uneven distance in the OFDM symbols. Finally, the arrangement used for these pilots is of the comb-type.

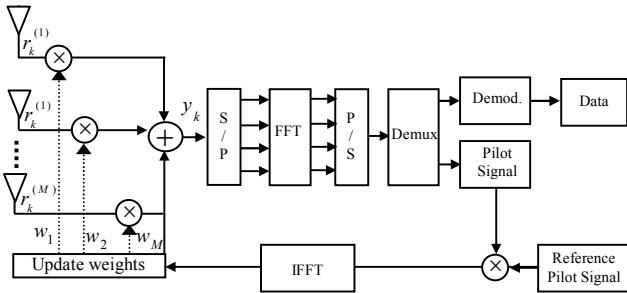


Fig.4: Pre-FFT array processing.

### 3.2. LMS Beamforming based on Post-FFT array processing

In this OFDM-AAA, the receiving OFDM symbols in each element are transferred into FFT processing. The output signals from different elements are weighted at each subcarrier and then combined. The signal  $y_{km}$ , which represents the weighted signal of the  $k$ th subcarrier and the  $m$ th element, is given by:

$$y_{km} = w_{km}^* \cdot x_{km} \quad (6)$$

where  $(\cdot)^*$  represents the complex conjugate,  $x_{km}$  represents the signals after FFT processing, and  $w_{km}$  represents the weights of the  $k$ th subcarrier and the  $m$ th element, respectively.

The array output of the  $k$ th subcarrier is given by:

$$y_k = \sum_{m=1}^M w_{km}^* \cdot x_{km} \quad (7)$$

For conventional systems, many algorithms to update the weights have been proposed. In this paper, the weight vector is updated by minimizing the MSE criterion using the LMS

algorithm. Fig.5 shows a typical architecture of post-FFT adaptive array processing presented in [12] without channel estimation.

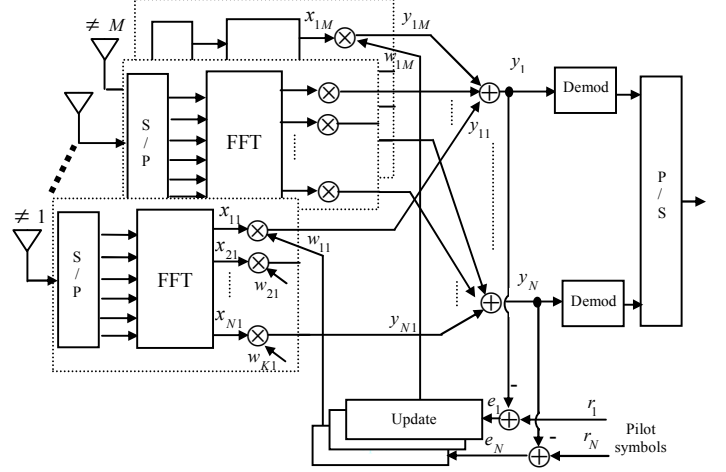


Fig.5: Post-FFT array processing.

The packet structure with block-type pilot arrangement is presented in Fig.6. Every packet is divided into pilot and data frames. The pilot frames are used to update to weight value of the beamforming for every subcarrier as shown fig 5. The values of these weights are maintained while receiving the data frames.

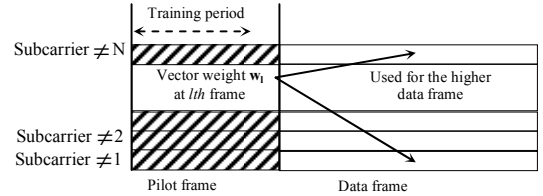


Fig.6: Packet Structure.

## 4. COMPUTER SIMULATION

### 4.1. Simulation results for Pre-FFT array processing

This section describes the performance and limitations of the pre-FFT-AA approach employed in several channel environments. The type-A channel is Rayleigh fading with a modified Poisson time-path-arrival distribution and a Doppler shift  $f_{d1}=20$ Hz. The type-B channel is Rayleigh fading with a modified Poisson time-path-arrival distribution and a higher Doppler shift  $f_{d2}=35$ Hz. Both these types of channel are studied for two rates  $R_1=12$ Mbps and  $R_2=18$ Mbps. The BER performance for different Doppler frequency values ( $f_{d1}=20$ Hz and  $f_{d2}=35$ Hz) were also studied. These two Doppler frequency values reflect the typical vehicle speeds of 10 and 15Km/h in our underground environment, respectively.

Table 1 summarizes the system parameters for the following computer simulation.

Table1: Simulation parameters.

Modulation method	DQPSK/OFDM
Nbr of subcarrier	52 (including 4 pilot subcarriers for pre-FFT only)
FFT/IFFT size	64
Length of guard interval	20% of symbol length (16 samples)
Antenna array type	Linear uniform
Nbr of antenna elements	4 elements
Element space	$\lambda/2$
Channel model	Amplitude: Rayleigh Time Path Arrival: Modified Poisson distribution
Adaptive algorithm	LMS
Max. Doppler frequency	20Hz and 35Hz
Packet size	20 symbols $\times$ 52 subcarriers
Frame size	96 samples
Pilot symbol	Pre-FFT: 4 pilot subcarriers Post-FFT: 2 pilot symbol OFDM
Rate	12Mbps and 18 Mbps
Carrier Frequency	$f_c=2.4\text{GHz}$
Noise	AWGN

OFDM is set up herein similarly to existing WLAN family standards, such as IEEE 802.11g. One OFDM symbol is composed of 80 samples, where the guard interval length is 16 and the useful symbol length is 64 samples. Here the OFDM symbol is generated with the 64-point IFFT, where only 48 subcarriers contain data information, 4 subcarriers are known pilot signals and other 12 subcarriers are virtual subcarriers (equal to zeros).

Figs. 7 and 8 show the BER performance of the pre-FFT adaptive array for the type-A channel environment for both rate values ( $R_1$  and  $R_2$ ), respectively, at 2.4 GHz and for different antenna numbers.

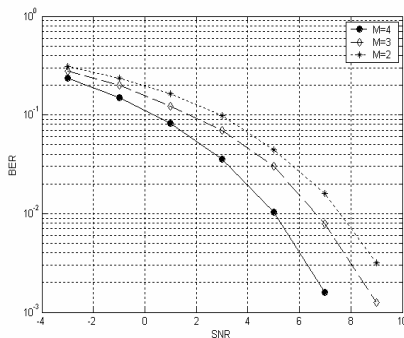


Fig.7: BER performance versus SNR for pre-FFT in Type-A Channel for  $R_1=12\text{Mbps}$  when the number of elements is varied.

Figs. 9 and 10 show the BER performance of the pre-FFT adaptive array for the type-B channel environment for both rate values ( $R_1$  and  $R_2$ ), respectively, at 2.4 GHz and for different antenna numbers.

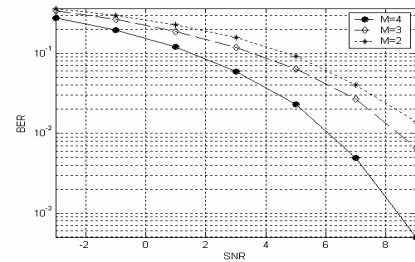


Fig.8: BER performance versus SNR for pre-FFT in Type-A Channel for  $R_2=18\text{Mbps}$  when the number of elements is varied.

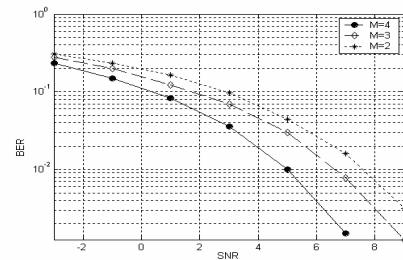


Fig.9: BER performance versus SNR for pre-FFT in Type-B Channel for  $R_1=12\text{Mbps}$  when the number of elements is varied.

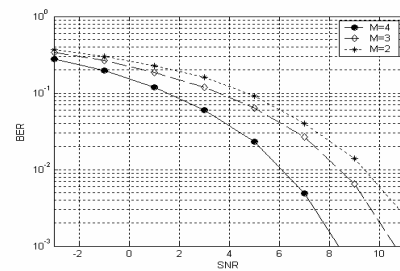


Fig.10: BER performance versus SNR for pre-FFT in Type-B Channel for  $R_2=18\text{Mbps}$  when the number of elements is varied.

Figures 7 to 10 demonstrate that the improvement in the BER performance is proportional to the number of elements exploited in the adaptation. From these results, it can be noted that this improvement decreases with an increase of the Doppler frequency.

When the rate increases, the period of the symbol decreases and hence generates more ISI. Indeed, some degradation of the BER performance is clearly seen in Figs. 8 and 10 compared to those in 7 and 9.

#### 4.2. Simulation results for Post-FFT array processing

The post-FFT array processing enables the use of several conventional diversity algorithms in the frequency domain of an OFDM system. Since each subcarrier is treated as an independent received signal, the diversity operation can be adopted for each individual subcarrier. This section studies the performance of the post-FFT-AA approach over the channels types-A and B and over two other kinds of channel environments (C, D). The type-C channel is Rayleigh fading with Doppler shift  $f_{d1}=20\text{Hz}$  while the type-D channel is Rayleigh fading with Doppler shift  $f_{d2}=35\text{Hz}$ .

Figs. 11 and 12 show the BER performance of the post-FFT adaptive array for different types of channel environments for rate values  $R_1$  and  $R_2$ , respectively, at 2.4 GHz. The number of antennas is  $M=4$ .

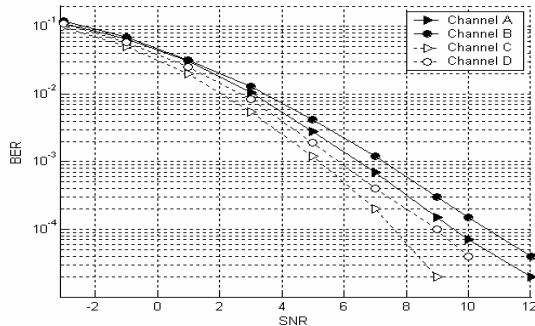


Fig.11: BER performance versus SNR for post-FFT for  $R_1=12$  Mbps for different type channels (A, B, C and D).

Figure 11 demonstrates that the improvement in BER performance decreases with larger Doppler frequencies and when the time path arrival has a modified Poisson distribution. Compared to types-C and D channels, the SNR degradation loss for types A and B channels are about 1.3 dB and 1.5 dB, respectively, for a required BER=0.001. Therefore, once the received signal has a significant Doppler shift, even when it arrives within the guard interval, it severely deteriorates the BER as inter-subcarrier interference.

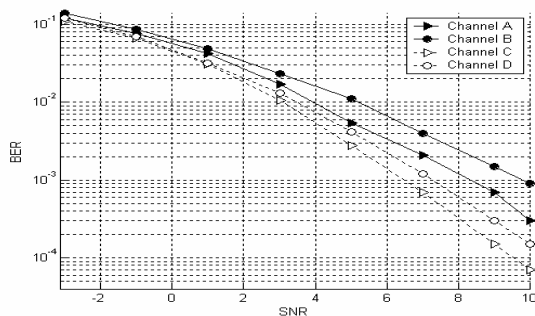


Fig.12: BER performance versus SNR for post-FFT for  $R_2=18$  Mbps for different type channels (A, B, C and D).

Figures 12 leads to a similar conclusion. Compared to types C and D channels, the SNR degradation loss for types A and B channels are about 1.5 dB and 2.5 dB, respectively, for a required BER=0.001. However, when the transmission rate increases, as illustrated in Fig. 12, the BER performance is clearly seen compared to the one in Fig.11.

Furthermore, large Doppler shift value and modified Poisson time path arrival can change the symbol length, so inter-symbol interference can be arise and deteriorate also the BER performance.

## 5. CONCLUSION

In this paper, the statistical modeling of propagation channel characteristics has been considered for a mining environment, and the impact of Rayleigh fading and modified Poisson distribution for the path arrival on WLAN OFDM-AAA

systems performance has also been investigated using both structures of OFDM- AAA, namely, pre-FFT and post-FFT array processing.

It is clear that the MMSE-AAA applied here to OFDM antenna array system reduces the Inter Carrier Interference (ICI) but not the inter-subcarrier interference. For this, the influence of the multipath characteristics (the distribution, the number and time delay difference) on BER performance has been studied. From this comparative study of antenna array architectures using pre-FFT and post-FFT array processing, the sensitivity to the distribution type of the multipath, fading channel, rate and Doppler frequency has been illustrated.

Simulation results show that the improvement in the BER performance decreases with an increase in the Doppler frequency value. In addition, if we operate at a high rate (or if we use for example high modulation order such as 16-QAM that operate at  $R=24$ Mbps), the access delay can be larger than the FFT sampling period, and then the ISI can be more severe.

Thus when a higher rate is needed, the pilots used for adaptation should be increased or advanced semi-blind and blind adaptive methods can be used to reduce overhead.

## REFERENCES

- [1] R.V. Nee, "A New OFDM standard for high rate wireless LAN in the 5 GHz band," in proc. 50<sup>th</sup> Vehicular Technology Conf. (VTC 99), vol. 1, Amsterdam, the Netherlands, Sept 99, pp. 256-262;
- [2] C.K Kim, K. Lee, and Y.S. Cho; "Adaptive beamforming algorithm for OFDM systems with antenna arrays", IEEE Trans. Consum. Electron., vol.46, No.4, Nov. 2000, pp.1052 – 1058;
- [3] Ari T. Alastalo and Mika Kahola; "Smart Antenna Operation for indoor Wireless Local Area Networks Using OFDM", IEEE Trans. On Wireless Comm., vol.2, No.2, March 2003, pp.392-399;
- [4] M. Boutin, S. Affes, C. Despins, T. Denidni; "Statistical Modelling of a Radio Propagation Channel in an Underground Mine at 2.4 and 5.8 GHz ", Proc. of IEEE VTC'05-spring;
- [5] A. Benzakour, S. Affes, C. Despins, and P.M. Tardif, "Wideband Measurements of Channel Characteristics at 2.4 and 5.8 GHz in Underground Mining Environments", Proc. of IEEE VTC'04-Fall, Los Angeles, California, USA, Sept. 26-29, 2004.
- [6] F. Maehara, F. Sasamori, and F. Takahata; "Inter-symbol interference suppression scheme using even-numbered sub-carriers for OFDM systems", Proc. IST Mobile & Wireless Comm. 2003. vol.1, June 2003, pp.83-87;
- [7] B.Canpolat and Y. Tanik; "Performance Analysis of Adaptive Loading OFDM Under Rayleigh Fading", IEEE Trans. On Vehicular Technology, vol.53, No.4, July 2004, pp.1105 – 1115;
- [8] S. Hara, M. Budsabathon, and Y. Hara; "A Pre-FFT OFDM Adaptive Antenna Array with Eigenvector Combining", IEEE Trans. Commun. Society, vol.46, No.4, Nov. 2000, pp.2412– 2416;
- [9] Y. G. Li and N.R. Sollenberger; "Adaptive Antenna arrays for OFDM system with co channel interference", IEEE Trans. Commun., vol.47, No.2, Feb. 1999, pp.217– 229.
- [10] E. Tufvesson and T Maseng, "Pilot assisted channel estimation for OFDM in mobile cellular- systems," in Proc. IEEE 47th Vehicular Technology Conference, Phoenix, USA, May 1997, pp. 1639-1643
- [11] T. Fujii and Y. Suzuki, "Two-Dimensional RLS OFDM adaptive Array Antenna Using Signals of adjacent Subcarriers", <http://www.suzuki-lab.tuat.ac.jp/member/fujii/pdf/wpmc03-wa10-1.pdf>
- [12] Hiramoto, T.; Mizuki, A.; Shibahara, M.; Fujii, T.; Sasase, I.; "Weight tracking method for OFDM adaptive array in time variant fading channel", Mobile and Wireless Comm. Network, 2002. 4th International Workshop on 9-11 Sept. 2002, pp.611 – 615.